

# Mössbauer investigation of the surface and volume spin-reorientation phase transition in Fe<sub>3</sub>BO<sub>6</sub>

A. S. Kamzin and L. A. Grigor'ev

A. F. Ioffe Physicotechnical Institute, Russian Academy of Sciences, 194021 St. Petersburg, Russia  
(Submitted 30 April 1993)

Zh. Eksp. Teor. Fiz. **104**, 3489–3511 (October 1993)

The surface spin-reorientational phase transition in a macroscopic antiferromagnetic Fe<sub>3</sub>BO<sub>6</sub> crystal with a weak ferromagnetic moment was investigated. The measurements were performed by means of simultaneous  $\gamma$ -ray, x-ray, and electron Mössbauer spectroscopy {A. S. Kamzin, V. P. Rusakov, and L. A. Grigor'ev in *Proceedings of Physics of Transition Metals*, 1988, Part 2, p. 271; A. S. Kamzin and L. A. Grigor'ev, *Pis'mas Zh. Tekh. Fiz.* **16**, 38 (1990) [Sov. Tech. Fiz. Lett. **16**, 417 (1990)]}, which makes it possible to study both the surface and volume properties of a bulk crystal. It was observed that 1) the first-order spin-reorientational transition observed in the volume of the crystal is accompanied by continuous reorientation of spins on the surface of the crystal; 2) toward the surface of the crystal the phase transition range becomes wider and no displacement of the center of the transition region is observed; 3) outside the transition region the direction of the magnetic moments on the surface is different from that in the volume of the crystal. The experimental data obtained agree qualitatively with the phenomenological theory of surface spin-reorientational phase transitions in macrocrystals {M. I. Kaganov, *Zh. Eksp. Teor. Fiz.* **79**, 1544 (1980) [Sov. Phys. JETP **52**, 779 (1980)]}.

## INTRODUCTION

There is now a great deal of interest in surface magnetic structure and surface phase transformations, since lowering the surface symmetry can induce new magnetic structures and interesting magnetic phenomena. Most investigations in this field concern transitions at the Curie point (order-disorder type),<sup>1,2</sup> because characteristic features of the phases—which make it possible to distinguish the phases easily—are observed above and below this transition point.

Significantly fewer experimental and theoretical investigations of magnetic structure and spin-reorientational phase transitions have been performed on the surfaces of macrocrystals.

Investigations of surface magnetic structure in  $\alpha$ -Fe<sub>2</sub>O<sub>3</sub> (Refs. 3 and 4) by means of measurements of the surface magneto-optic Kerr effect have led to the conclusion that the antiferromagnetism vector on the (100) and (111) faces at temperatures above the Morin spin-reorientational transition point tilts out of the basal plane. In ErFeO<sub>3</sub> (Ref. 5) and TbFeO<sub>3</sub> (Ref. 6) strong (compared to the volume transition) upward displacement of the temperature (to 40 K of the onset of  $G_x F_z \leftrightarrow G_z F_x$  reorientation was observed at the surface. In addition, if  $G_x F_z \leftrightarrow G_z F_x$  spin orientation occurs in the interior of TbFeO<sub>3</sub>,<sup>7</sup> then a  $G_x F_z \leftrightarrow G_y$  Morin transition occurs in the surface layer.<sup>6</sup> Therefore, as conjectured in Ref. 6, a transitional layer exists on the surface of a TbFeO<sub>3</sub> crystal in which the antiferromagnetism vector rotates by 90° ( $G_x \rightarrow G_y$ ) and the ferromagnetism vector decreases in magnitude from  $F_z$  to zero. In Refs. 8 and 9 a macroscopic transitional magnetic layer was observed on the surface of FeBO<sub>3</sub>.

In the opinion of G. S. Krinchik *et al.*,<sup>3,4</sup> in both he-

matite and rare-earth orthoferrites surface magnetism is observed near the spin-reorientational phase transition, i.e., where the first anisotropy constant  $k_1$  changes sign and is small in magnitude, and therefore surface anisotropy cannot compete with bulk anisotropy. On the other hand, surface magnetism in hematite has been explained successfully only by taking into account the change in the Fe-Fe magnetic-dipole interaction in the surface layer.<sup>3</sup> In the case of rare-earth orthoferrites it was found that the interaction of different types of R-Fe bonds must be taken into account.<sup>5,6</sup>

Mössbauer spectroscopy is an effective method for investigating spin-reorientational phase transitions, since it enables the direction of orientation of the spin magnetic moments, to be determined directly. Mössbauer investigations have shown that the surface and volume spin-reorientational transition temperatures in  $\alpha$ -Fe<sub>2</sub>O<sub>3</sub> are identical to within the measurement error ( $\pm 5$  K).<sup>10</sup> In Ref. 11 it was observed that the surface spin-reorientational transition temperature in  $\alpha$ -Fe<sub>2</sub>O<sub>3</sub> is several degrees higher than the volume transition temperature. In Refs. 12 and 13 Mössbauer investigations showed that the surface and volume spin-reorientational transition temperatures in Fe<sub>3</sub>BO<sub>6</sub> are in the same range [a first-order reorientational transition is observed in the volume of Fe<sub>3</sub>BO<sub>6</sub> (Ref. 14)].

In theoretical investigations the spin-reorientational phase transitions are described in the simplest case by introducing an effective anisotropy constant  $k_1$  which changes sign as the temperature changes.<sup>15,16</sup> The anisotropy energy can be written in the form

$$\Phi(\theta) = -k_1 \sin^2 \theta - k_2 \sin^4 \theta + C(\nabla\theta)^2. \quad (1)$$

Here  $k_1 = k_2(\tau)$ , where  $\tau = (T - T_R)/T_R$  and  $T_R$  is the

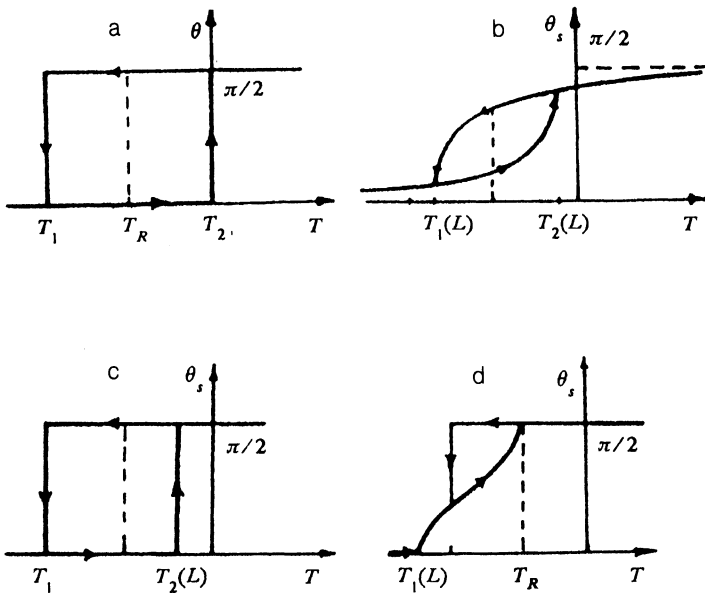


FIG. 1. Theoretical<sup>16</sup> plots of the angle  $\theta$  versus the temperature for a first-order spin-reorientational phase transition in the volume (a) and at the surface (b) of the crystal: b— $\varphi \neq 0, \pi/2$ ; c— $\varphi = 0, \pi/2$ , surface energy measure  $\sigma < 1$ ; d— $\varphi = 0, \pi/2$ ,  $\sigma > 1$ .

transition temperature in the interior;  $C \sim (T/\mu M_0)a^2$  is the inhomogeneous exchange interaction constant, where  $a$  is the interatomic distance,  $M_0$  is the saturation magnetic moment,  $\mu$  is the Bohr magneton, and  $T_C$  is the Curie temperature;  $k_2$  is the second anisotropy constant ( $|k_2| \ll |k_1|$  far from  $T = T_R$ ); and  $\theta$  is the angle between the magnetic moment and one axis of the crystal (order parameter). The character of the volume transition is determined by the sign of  $k_2$ : For  $k_2 > 0$  the transition from the state  $\theta = 0$  into the state  $\theta = \pi/2$  occurs abruptly, as a first-order transition. At  $T = T_R$ , where  $T_R$  is determined by the condition that the thermodynamic potentials of both phases be equal, i.e., by the equation  $k_1(\tau) - k_2 = 0$ , the temperatures  $T_1$  and  $T_2$  are determined by the equations  $k_1(\tau_2) = 0$  and  $k_1(\tau_1) + 2k_2 = 0$ , i.e., the phase with  $\theta = 0$  loses its lability at  $k_1 = 0$  or  $T = T_2$ , and the phase with  $\theta = \pi/2$  loses its lability at  $k_1 = -2k_2$  or  $T = T_1$ . The temperature dependence of the angle  $\theta$  for such a case is shown in Fig. 1a.

In his theoretical investigations of surface reorientational phase transitions in bulk crystals, Kaganov<sup>16</sup> introduced, in addition to the angle  $\theta_S$  determining the orientation of the magnetic moments in the volume, a new parameter  $\varphi$  which determines the direction of the easy-magnetization axis at the surface of the crystal. Next, he conjectured that not only can the magnitude of the anisotropy constant change at the surface, but the direction of the easy and difficult magnetization axes can also change. With the help of the new parameter  $\varphi$ , which gives the direction of the easy-magnetization axis on the surface for  $k_S > 0$ , when the magnetic moments both on the surface and in the interior are parallel to the surface plane of the sample, the surface energy was represented in the form

$$f_S = k_S \sin^2(\theta_S - \varphi), \quad (2)$$

where  $k_S$  is the surface anisotropy constant,  $\theta_S$  is the value

of the angle  $\theta$  on the surface of the sample, and the angle  $\varphi$  gives the direction of the easy-magnetization axis at the surface for  $k_S > 0$ .

In Ref. 16 Kaganov used these assumptions to study the mechanisms of surface spin-reorientational transition for the cases when a first-order phase transition (spin reorientation is abrupt) or a second-order transition (spin reorientation is continuous) is observed in the volume of the crystal, depending on the orientation of the easy axis at the surface of the crystal, i.e., depending on the parameter  $\varphi$ . Since a first-order phase transition occurs in the volume of the  $\text{Fe}_3\text{BO}_6$  crystal with which we are concerned, we shall examine the results obtained in Ref. 16 for this case.

For  $\varphi \neq 0$  or  $\pi/2$ , as shown in Ref. 16, first, the angle  $\theta_S$  at the surface of the sample is always different from zero and  $\pi/2$  and, second, the  $\theta_S$  hysteresis loop is narrower than in the interior of the sample (Fig. 1b).

According to the calculations in Ref. 16, in the case  $\varphi = \pi/2$  (analogously to  $\varphi = 0$ ) the disadvantageous (from the standpoint of surface energy) state with  $\theta_S = 0$  for  $\varphi = \pi/2$  can become unstable before the potentials of the  $\theta_S = 0$  and  $\theta_S = \pi/2$  phases become equal (Fig. 1c). Reorientation at the surface starts with a second-order phase transition at the point  $k_{1c} = -k_2\sigma^2$  or  $T = T_1(L)$  ( $\sigma$  is a measure of the surface energy), where an intermediate surface state appears. The transition from it into the  $\theta_S = \pi/2$  phase is always a first-order transition, but it can be accompanied by a jump in  $\theta_S$  or it can occur continuously (see Fig. 1d).

A phenomenological theory of spin-reorientational phase transitions in plates was constructed in Ref. 17. It was shown that if a first-order phase transition occurs in the volume of the crystal, then for a definite critical thickness of the plate in the case when the easy axis is oriented on the surface at an angle to the plane of the surface ( $\varphi \neq 0$  or  $\pi/2$ ) the temperature-hysteresis loop collapses. For



# 1. METHOD OF SIMULTANEOUS $\gamma$ -RAY, X-RAY, AND ELECTRON MÖSSBAUER SPECTROSCOPY OF THE SURFACE AND VOLUME OF MACROSCOPIC CRYSTALS

The method of simultaneous  $\gamma$ -ray, x-ray, and electron Mössbauer spectroscopy proposed in Ref. 12 and described in Ref. 19 was used for the investigations. This method enables investigation of the surface and volume properties of macroscopic crystals.

The method is based on the fact that  $\gamma$  rays, characteristic x-rays, and conversion and Auger electrons (secondary electrons), all of which are employed for observing the Mössbauer effect, have different ranges in matter. It is well known<sup>20</sup> that when  $^{57}\text{Fe}$  is used and the  $\gamma$ -rays are recorded in a geometry such that the rays pass through the sample being investigated, i.e., the conventional method of Mössbauer spectroscopy, the most convenient crystals for investigations of bulk properties have thicknesses from tens to hundreds of microns. The use of Mössbauer spectroscopy with detection of characteristic x-rays allows the properties of a  $\sim 10 \mu\text{m}$  thick layer of a bulk crystal to be studied. In the case when Mössbauer spectroscopy is used together with detection of secondary electrons, the information is extracted from a 300 nm surface layer on the bulk sample.

The method of simultaneous  $\gamma$ -ray, x-ray, and electron Mössbauer spectroscopy proposed in Ref. 12 combines these three modifications of Mössbauer spectroscopy and makes it possible to obtain the spectra immediately by recording the  $\gamma$  rays, characteristic x-rays, and secondary electrons with the help of the universal detector described in Ref. 19 and 21, thereby simultaneously studying the properties of the volume and surface layers of a bulk crystal. The universal detector proposed in Refs. 19 and 21 makes it possible to perform such measurements at temperatures ranging from 100 to 750 K. This method of investigation was later called simultaneous triple radiation Mössbauer spectroscopy.<sup>22</sup>

The spectrometer constructed around the universal detector is displayed in Fig. 2. The proportional counters  $\Gamma$ , X, and E of the universal detector record  $\gamma$ -rays, x-rays, and secondary electrons, respectively. The signals from the counters are fed through the amplification (A) and discrimination (D) channels into the corresponding accumulators (ACC) of the Mössbauer spectra. The sample (S) is placed on a heater (H). The temperature is maintained constant with an accuracy better than 0.2 K. The form of the motion of the  $\gamma$ -ray source is prescribed on the vibrator (V) by a generator (G). The spectrometer is controlled with the help of a computer in the dialogue mode. The spectrometer is described in detail in Ref. 23.

In the present work it was necessary to investigate surface layers less than 300 nm thick, and for this reason the resolution of the counter E (See Fig. 2) was increased significantly.<sup>24</sup> This was achieved by using a thinner anode than in Ref. 20 and by decreasing the distance between the sample and the anode. As shown in Ref. 24, together with the help of a proportional counter, this made possible selection of secondary electrons by energies. It is well known

that the energy of an electron which has penetrated into the sample decreases as a function of the depth of the layer in which this electron was formed. By recording the electrons in a definite energy group and taking into account the probability that an electron reaches the surface of the crystal, it is possible to investigate the properties of a thin layer located at a definite depth from the surface. When a proportional detector is employed, the location of the layer and its thickness are not determined as accurately as with the electrostatic or magnetic energy analyzers, with which narrow sections can be cut out of the energy spectrum of the electrons which are produced, for example, in the conversion  $K$  transition. However, a proportional detector is much more efficient, and this has certain advantages.<sup>20</sup>

Thus the spectrometer employed in the present work makes it possible by selecting electrons by energy with the help of discriminators, to obtain Mössbauer spectra of a  $50 \pm 10 \text{ nm}$  thick layer located about 300 nm from the surface and spectra from the interior of a sample by recording  $\gamma$ -rays and x-rays. Another important advantage of the method of simultaneous Mössbauer spectroscopy<sup>12</sup> is that the information from the interior and surface of a macroscopic crystal is extracted under identical conditions.

## 2. MÖSSBAUER INVESTIGATIONS OF SPIN-REORIENTATIONAL PHASE TRANSITIONS

The arrangement of the hyperfine sublevels is determined by the ratio of the magnetic and electric interaction

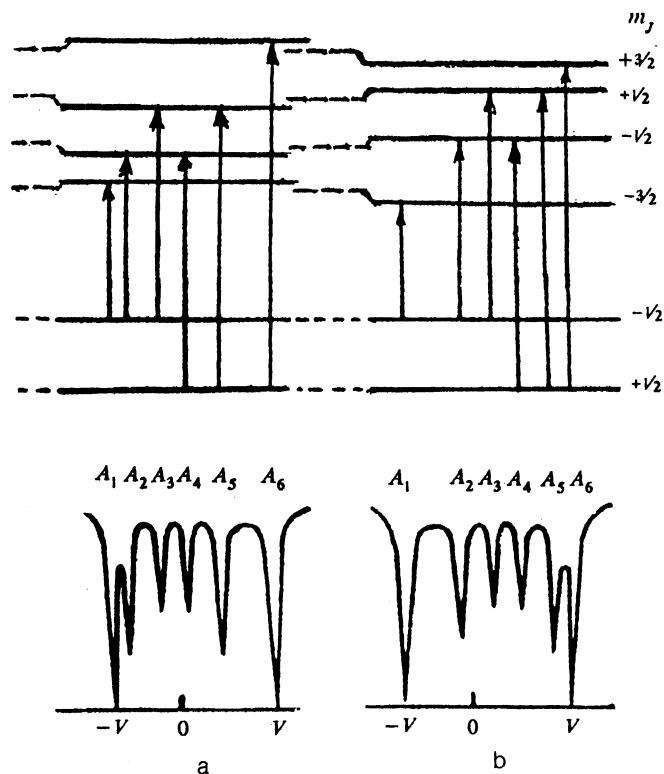


FIG. 3. Characteristic arrangements of the energy levels of  $^{57}\text{Fe}$  nuclei (top) and the corresponding Mössbauer absorption spectra (bottom).

energies, by the symmetry of the electric-field gradient, and in the general case by the orientation of the internal magnetic field with respect to the axes of the electric-field-gradient tensor.<sup>25,26</sup> If the magnetic hyperfine interaction energy is significantly higher than the electric interaction energy, then the sublevels of the excited state of the spin-3/2 nucleus are shifted in the manner shown in Fig. 3. The arrangement of the sublevels and correspondingly the positions of the lines in the Mössbauer spectrum along the ordinate depends on the angle  $\theta$  between the principal symmetry axis of the axisymmetric electric-field-gradient tensor and the direction of the effective magnetic field  $H_{\text{eff}}$  at the  $^{57}\text{Fe}$  nucleus. The orientation of  $H_{\text{eff}}$  is determined by the direction of the magnetic moment ( $\mathbf{M}$ ) of the iron ion. Assume that the principal symmetry axis of the axisymmetric field-gradient tensor is parallel to the crystallographic  $a$  axis and the arrangement of the sublevels applies to the case  $\theta = \pi/2$  in Fig. 3a and the case  $\theta = 0$  in Fig. 3b, i.e., to the sublevels observed below and above, respectively, the spin-reorientation region. The Mössbauer spectra observed on polycrystalline samples are displayed in Fig. 3.

When the investigation is performed on a single-crystalline plate whose crystallographic  $a$  axis is parallel to the normal to the plate surface and the direction of propagation of the  $\gamma$ -ray beam the intensity ratio of the component of the Zeeman sextuplet  $A_1:A_2:A_3:A_4:A_5:A_6$  depends on the angle between the direction of propagation of the wave vector of the  $\gamma$  rays and the magnetic moment of the iron ion (in this case, the angle  $\theta$ ) as follows:

$$\begin{aligned} &3(1 + \cos^2 \theta):4 \sin^2 \theta:(1 + \cos^2 \theta): \\ &(1 + \cos^2 \theta):4 \sin^2 \theta:4(1 + \cos^2 \theta). \end{aligned} \quad (3)$$

In the Mössbauer spectroscopy of single crystals the type of spin reorientational phase transition is determined with the help of a formula that relates the intensity of the second ( $A_2$ ) or fifth ( $A_5$ ) lines of the sextuplet corresponding to transitions with  $\Delta m = 0$  to the intensity of the first ( $A_1$ ) or sixth ( $A_6$ ) lines of the Zeeman sextuplet

$$A_{2,5}/A_{1,6} = 4 \sin^2 \theta / 3 (\cos^2 \theta + 1), \quad (4)$$

and by studying the temperature dependence of this ratio.

### 3. OBJECT OF INVESTIGATIONS

A  $\text{Fe}_3\text{BO}_6$  crystal, which below the Néel temperature (508 K) is an antiferromagnet with a weak ferromagnetic moment, was chosen for the investigations. The magnetic structure of  $\text{Fe}_3\text{BO}_6$  is formed by iron ions occupying two nonequivalent positions  $8d$  and  $4c$  in octahedral positions.<sup>27</sup> The number of iron ions in the  $4c$  positions is half the number of ions in the  $8d$  positions. As the temperature increases, a  $G_z F_x \leftrightarrow G_x F_z$  spin-reorientational phase transition is observed in  $\text{Fe}_3\text{BO}_6$  at  $T_R \approx 115$  K, and spin reorientation occurs in a narrow temperature range (less than 1 K).<sup>28</sup> In the reorientation process the magnetic moments rotate from the  $c$  axis to the  $a$  axis, the orientation of the weak ferromagnetic moment changing in

the process from the  $a$  axis ( $\Gamma_2$  phase) to the  $c$  axis ( $\Gamma_3$  phase). Such a phase transition is common in orthoferrites.<sup>15</sup>

The magnetic properties of  $\text{Fe}_3\text{BO}_6$  have been investigated in a large number of works. Many authors have tried to determine the mechanism of spin reorientation in  $\text{Fe}_3\text{BO}_6$  (see citations in Ref. 14), but it was shown convincingly only in Ref. 14 that the rotation of the magnetic moments occurs abruptly, as a first-order phase transition, and falls within some temperature range in which the low-temperature phase ( $\Gamma_2$ ) coexists with the high-temperature phase ( $\Gamma_3$ ), i.e., the intermediate state described in Ref. 29.

In Ref. 30 a new type of reorientational phase transition, previously unobserved in magnetic materials, was observed in  $\text{Fe}_3\text{BO}_6$ . This phase transition is associated with the fact that as the temperature increases, in the region  $\approx 490$  K the magnetic moments of one antiferromagnetic sublattice ( $4c$ ) rotate while the orientation of the moments in the other sublattice ( $8d$ ) remains unchanged right up to  $T_N$ .

As shown in Ref. 14, in the case of  $\text{Fe}_3\text{BO}_6$  there are a number of favorable circumstances which make it possible to interpret the experimental spectra correctly and with high accuracy. This is connected with the fact that the parameters of the hyperfine structure (effective magnetic fields, quadrupole splittings, and intensities of the resonance lines) of iron ions occupying  $8d$  and  $4c$  positions are different. In addition, the lines corresponding to the phases  $\Gamma_2$  and  $\Gamma_3$  can be resolved because the parameters of the hyperfine structure in these phases differ significantly. For this reason, although the experimentally observed spectra near  $T_R$  consist of sextuplets correspond to two nonequivalent magnetic sublattices  $8d$  and  $4c$  found in both the  $\Gamma_2$  and  $\Gamma_3$  phases, the lines referring to different sublattices ( $8d$  and  $4c$ ) and states of the crystal ( $\Gamma_2$  and  $\Gamma_3$ ) can be separated reliably.<sup>14</sup>

It could be conjectured on the basis of what was said above that the method first employed in Ref. 12 and described in Ref. 19 as well as a number of favorable properties<sup>14</sup> of the  $\text{Fe}_3\text{BO}_6$  crystals make it possible to study spin reorientation transitions in a thin surface layer of a bulk crystal, to make comparisons to the reorientation of magnetic moments in the volume, and to answer the following questions:

- 1) Does the rotation of the magnetic moments at the surface (just as in the interior) occur as a first-order phase transition, i.e., do they "flip" from one crystallographic direction to another abruptly, or do the spin moments at the surface rotate continuously from one crystallographic axis to another?
- 2) Are the limits of the surface phase transition different from those of the bulk transition?
- 3) Does the phase transition temperature change at the surface, i.e., does reorientation occur at the same temperature or at a different temperature compared to the volume?
- 4) How well do the experimental results agree with

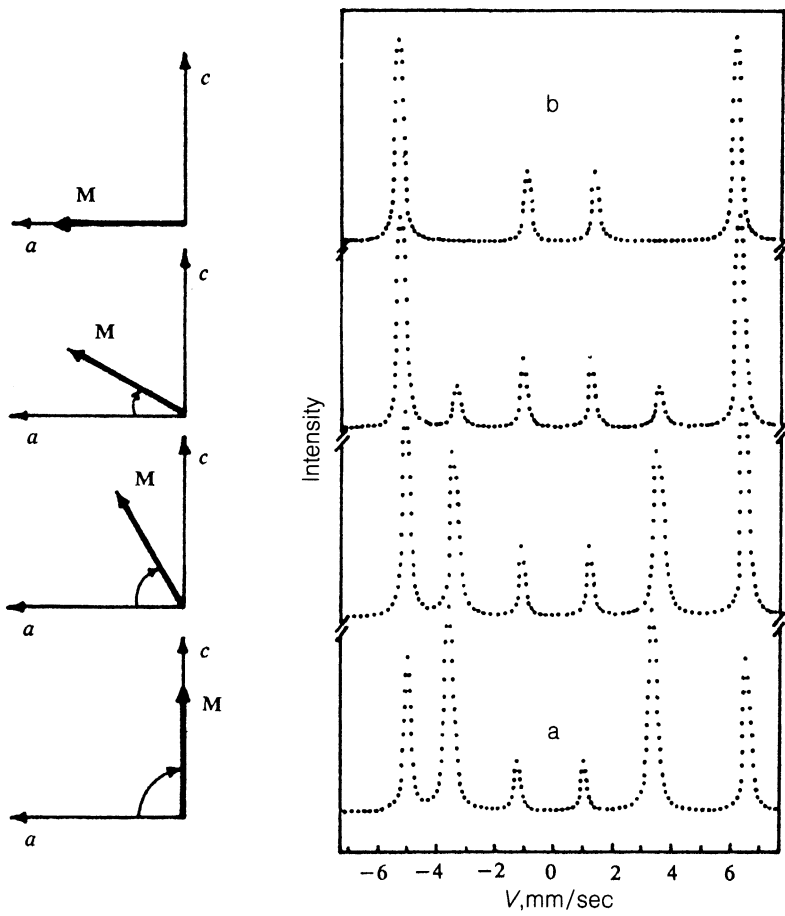


FIG. 4. Reorientation of the magnetic moments (left) and theoretical Mössbauer spectra (right) observed at a second-order spin-reorientational phase transition.

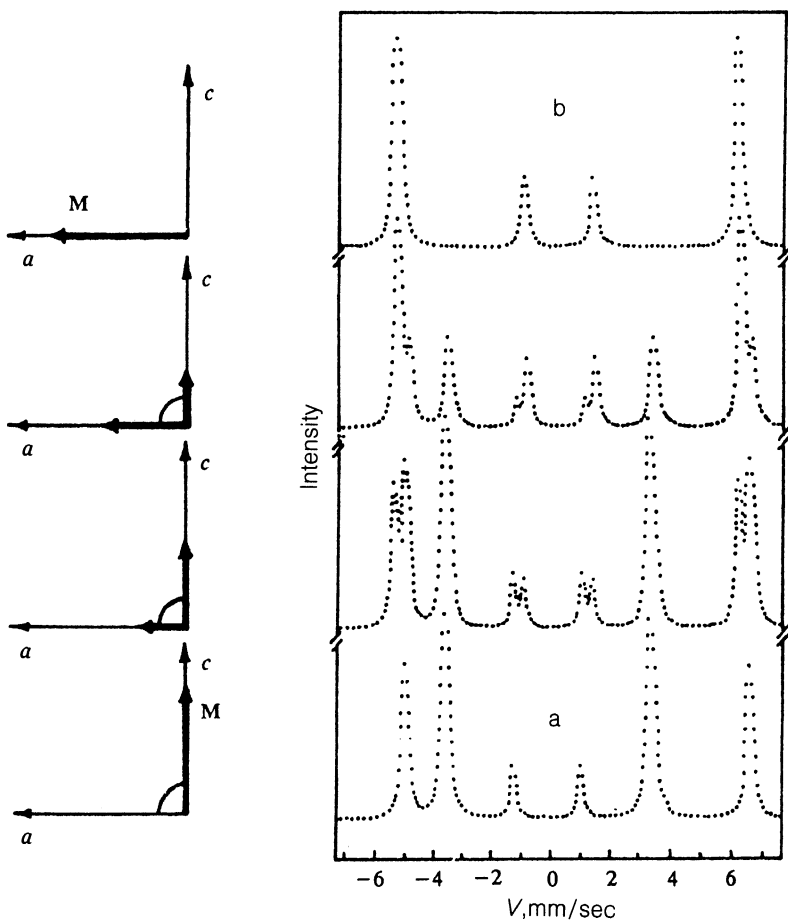


FIG. 5. Reorientation of the magnetic moments (left) and theoretical Mössbauer spectra (right) observed at a first-order spin-reorientational phase transition with formation of a nonuniform state.

theoretical investigations of surface spin-reorientational phase transitions?

The surface investigations were performed on single-crystalline plates with a thickness of about 120  $\mu\text{m}$ . The crystallographic  $a$  axis was directed perpendicular to the surface of a plate. Single crystals were prepared by two methods for surface studies: 1) mechanical polishing using fine polishing powders and light etchants and 2) chemical polishing in a 1:1 mixture of the acids  $\text{H}_3\text{PO}_4$  and  $\text{H}_2\text{SO}_4$  at room temperature for  $\sim 50$  h. Note that the experimental results were reproducible only in the second case.

#### 4. EXPERIMENTAL INVESTIGATIONS OF SURFACE AND BULK SPIN-REORIENTATIONAL TRANSITION IN THE ANTIFERROMAGNET $\text{Fe}_3\text{BO}_6$

##### 4.1 Details of the Mössbauer studies of the spin-reorientational transitions

Investigations of phase transitions by the method of Mössbauer spectroscopy are described in a number of reviews and monographs.<sup>31,32</sup> The possibilities of this method for studying reorientational transitions have nonetheless not been adequately explored. Note that if a first-order transition occurs in some temperature range [as happens in  $\alpha\text{-Fe}_2\text{O}_3$  (Refs. 33 and 34) or  $\text{Fe}_3\text{BO}_6$  (Ref. 14)], then significant details arise which could lead the experimenter to an erroneous conclusion about the type of phase transition.

As an example we consider the situation when reorientation of the spin magnetic moments with increasing temperature occurs from the crystallographic  $c$  axis to the  $a$  axis and we analyze the Mössbauer spectra for a single-crystalline plate in which the  $a$  axis is collinear with the normal to the surface of the plate.

In the case of a second-order phase transition the magnetic moments rotate continuously from the  $c$  axis to the  $a$  axis and the angle  $\theta$  also varies continuously, as shown in Fig. 4 (left-hand column). The magnetic sublevels of the excited state will be gradually displaced from the positions displayed in Fig. 3a into the positions displayed in Fig. 3b. The lines in the Mössbauer spectrum, as shown in Fig. 4, also shift continuously from a to b positions and the experimental spectrum at any point of the spin reorientation region consists of a single sextuplet (see Fig. 4a). The existence of a temperature gradient in the sample leads only to increase the spectral width. The intensities of the second and fifth lines in the sextuplet, corresponding to transitions with  $\Delta m = 0$ , gradually decrease to zero in the region of the transition as the angle  $\theta$  changes from  $90^\circ$  to  $0^\circ$ .

In the case of a first-order phase transition, as the temperature increases, the magnetic moments rotate abruptly from the  $c$  to the  $a$  axis and the angle  $\theta$  takes on only two values—0 or  $\pi/2$ . Therefore, the magnetic sublevels of the excited state can occupy only the two positions shown in Figs. 3a and 3b and the transition from one position into the other occurs abruptly. As shown in Fig. 5, the positions of the lines in the Mössbauer spectrum also change abruptly from a to b.

If the spin-reorientational transition occurs simultaneously in the entire crystal, i.e., the magnetic moments reorient abruptly as a whole, then just as in the preceding case, the experimental Mössbauer spectrum consists of a single Zeeman sextuplet, observed before and after the transition. The orientations of the magnetic moments and

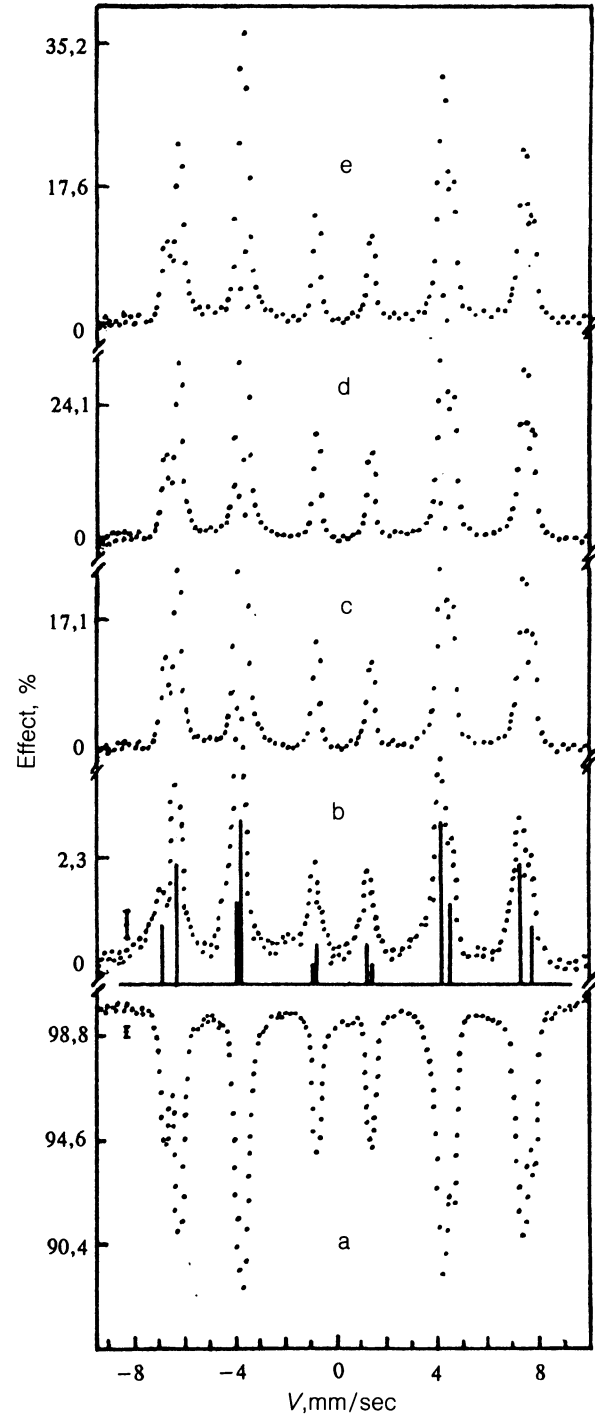


FIG. 6.  $\text{Fe}_3\text{BO}_6$  Mössbauer spectra obtained at  $T = 300 \text{ K} < T_R$  by recording  $\gamma$ -rays (a), x-rays (b), and electrons (c-e) from the interior (a,b) and the surface layers of thickness from 0 to 40 nm (c), 50 to 90 nm (d), and 150 to 200 nm (e). The positions and thickness of the layer are determined to within 20%. The line positions are indicated by the solid lines.

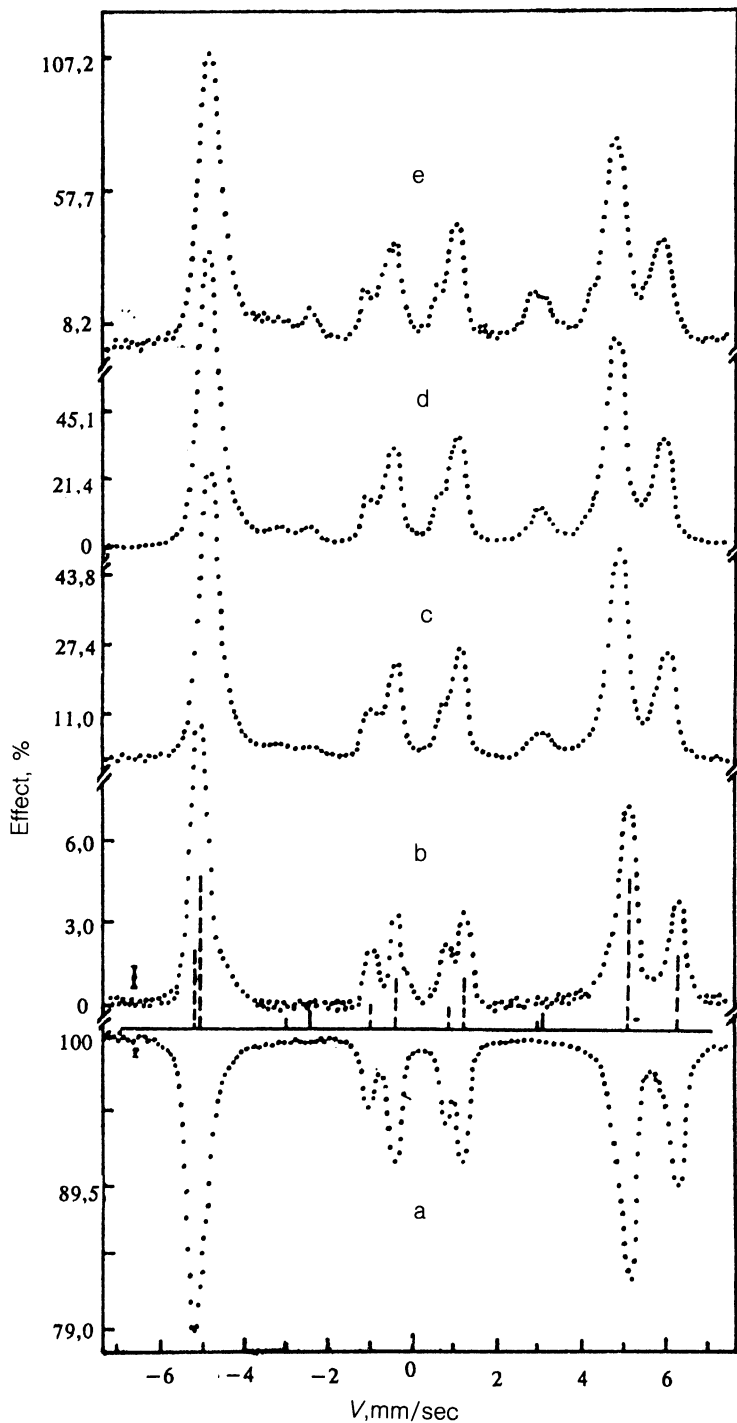


FIG. 7.  $\text{Fe}_3\text{BO}_6$  Mössbauer spectra obtained at  $T=427.3$  K  $> T_R$  by recording  $\gamma$ -rays (a), x-rays (b), and electrons (c-e) from the interior (a,b) and surface layers from 0 to 40 nm (c), 50 to 90 nm (d), and 150 to 200 nm (e). The location and thickness of the layers are determined to within 20%. The line positions are indicated by the dashed lines.

the form of the Mössbauer spectra are displayed in Fig. 5 (bottom and top).

In the case when the first-order transition occurs in some temperature range with formation of an intermediate state, domain structure is observed in the crystal. The antiferromagnetism vector in some domains is oriented along the  $a$  axis, while in other domains it is oriented along the  $c$  axis, i.e., the orientation differs by  $\pi/2$ . The relative number of these domains depends on the temperature, as shown in Fig. 5 (left side). The spectrum observed in this case consists of a superposition of the spectra from regions of the crystal where the magnetic moments have orthogonal

orientations, i.e., they consist of two sextuplets (Fig. 5). However, the intensities of the first and fifth lines of the Zeeman sextuplet, which correspond to transitions with  $\Delta m=0$ , decrease continuously to zero with increasing temperature in the region of the transition (for  $\theta=0$ ), just as in the preceding case of the second-order phase transition.

Thus in order to establish the type of spin-reorientational transition it is necessary not only to analyze the ratio of the line intensities of the Zeeman sextuplet (which is usually done) but also to investigate how the positions of the resonance lines in the region of the transition change—continuously or abruptly. Otherwise the for-

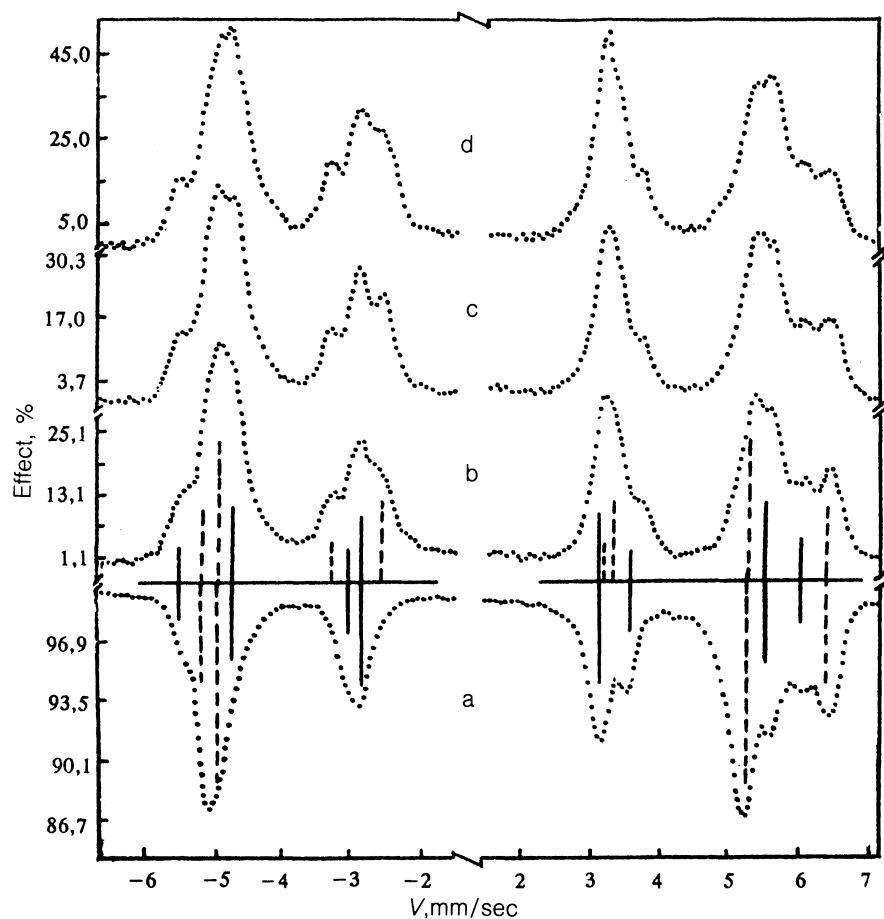


FIG. 8.  $\text{Fe}_3\text{BO}_6$  Mössbauer spectra obtained in the temperature range of the spin-reorientational phase transition  $T_1(L) < T = 416 \text{ K} < T_2(L)$  by recording  $\gamma$ -rays (a) and electrons (b-d) from the volume (a) and surface layers from 0 to 40 nm (b), 50 to 90 nm (c), and 150 to 200 nm (d). The location and thickness of the layers are determined to within 20%.

mation of an inhomogeneous state at a first-order phase transition can be misinterpreted as a second-order phase transition.

#### 4.2 Results of experimental investigations of spin-reorientational phase transitions in $\text{Fe}_3\text{BO}_6$

The experimental Mössbauer spectra, obtained by recording  $\gamma$ -rays, x-rays, and secondary electrons at temperatures below and above the phase transition point as well as in the region of the transition, are displayed in Figs. 6–8.

Analysis of the spectra obtained in the temperature range below 450 K showed that depending on the depth ( $L$ ) of the layer investigated, three characteristic temperature regions can be distinguished: I— $T < T_1(L)$ ; II— $T > T_2(L)$ ; III— $T_1(L) < T < T_2(L)$ .

In the region I the spectra obtained by recording  $\gamma$ -rays and x-rays and shown in Figs. 6a and b consist of a superposition of two Zeeman sextuplets, corresponding to iron ions occupying  $8d$  and  $4c$  positions. The line intensities in each sextuplet are in the ratio 3:4:1:1:4:1, which indicates that the spin magnetic moments of the iron ions are perpendicular to the direction of the  $\gamma$ -ray beam. This means that the magnetic moments are parallel to the crystallographic  $c$  axis ( $\Gamma_2$  phase). The numerically determined positions of the lines are displayed in Fig. 6 (solid lines). The lines referring to the iron ions in the  $8d$  positions are twice as strong as the lines referring to the iron ions in the  $4c$  positions.

The Mössbauer spectra obtained from surface layers by recording the secondary electrons are displayed in Figs. 6c, d, and e. Analysis of the electron spectra displayed in Fig. 6 showed that the line-intensity ratios of the sextuplets are not 3:4:1:1:4:3. This indicates that the spin magnetic moments deviate from directions orthogonal to the wave vector of the  $\gamma$ -ray beam.

In region II the experimental spectra obtained by recording  $\gamma$ -rays and x-rays, as seen from Fig. 7a and b, consist of two Zeeman sextuplets, whose positions are shown in Fig. 7 by the dashed lines. The line intensities in the sextuplets are in the ratio 3:0:1:1:0:3. The absence of the second and fifth lines of the sextuplet, which correspond to transitions with  $\Delta m = 0$ , indicates that in the temperature range studied the spin magnetic moments of the iron ions are parallel to the direction of the  $\gamma$ -ray beam, and correspondingly, the crystallographic  $c$  axis. Thus the bulk of the crystal is in the  $\Gamma_3$  phase.

The Mössbauer spectra obtained by recording secondary electrons in the region II are displayed in Figs. 7c, d, and e. Analysis of the spectra reveals that the second and fifth lines of the sextuplet, which correspond to transitions with  $\Delta m = 0$ , do not vanish at the temperature  $T_2(L)$ , but rather decrease continuously to zero in some temperature range above  $T_2(L)$ .

In the region III, in the temperature range  $T_1(L) < T < T_2(L)$ , the experimental spectra obtained by recording the  $\gamma$ -rays and x-rays are a superposition of the

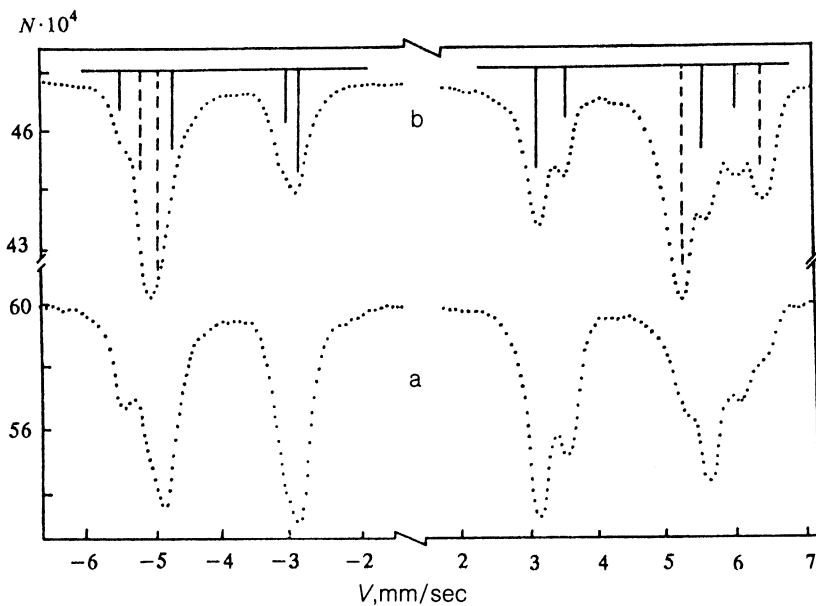


FIG. 9.  $\text{Fe}_3\text{BO}_6$  Mössbauer spectra near  $T_R$  obtained by recording  $\gamma$ -rays at temperatures 415 K (a) and 416 K (b).

spectra observed at temperatures below  $T_1$  and above  $T_2$ , i.e., lines belonging to the  $\Gamma_2$  and  $\Gamma_3$  phases are present simultaneously in the spectra. As an example, Fig. 8a displays the experimental spectrum obtained by recording  $\gamma$ -rays in the temperature range discussed. In order to facilitate interpretation, the x-ray Mössbauer spectrum is not shown in Fig. 8 (it is similar to the  $\gamma$ -ray spectrum). The positions of the Zeeman lines corresponding to the  $\Gamma_2$  and  $\Gamma_3$  phases differ significantly. Thus it is possible to determine reliably from the spectra the magnetic phase ( $\Gamma_2$  or  $\Gamma_3$ ) to which the observed lines belong. This is seen well in Fig. 8, where these lines are displayed on an enlarged velocity scale. The ratio of the line intensities in the sextuplets indicates that the spin magnetic moments of the iron

ions are oriented along the  $c$  axis ( $\Gamma_2$  phase) and the  $a$  axis ( $\Gamma_3$  phase). As the temperature increases from  $T_1$  to  $T_2$ , the absorption lines abruptly shift from positions corresponding to the  $\Gamma_2$  phase into positions corresponding to the  $\Gamma_3$  phase. At  $T_1$  the lines belonging to the  $\Gamma_2$  phase become weaker and at  $T_2$  the lines belonging to the  $\Gamma_2$  phase vanish. At  $T_1$  lines belonging to the  $\Gamma_3$  phase appear in the spectra, and becoming stronger as the temperature increases from  $T_1$  to  $T_2$ . This is seen well in the sections of the spectra corresponding to the first and second (fifth and sixth) lines of the Zeeman sextuplet, displayed in Fig. 9. At temperatures from  $T_1$  to  $T_2$  lines of the Zeeman sextuplets of both phases are always present. Analysis of the second and fifth lines of the Zeeman sextuplets reveals that at

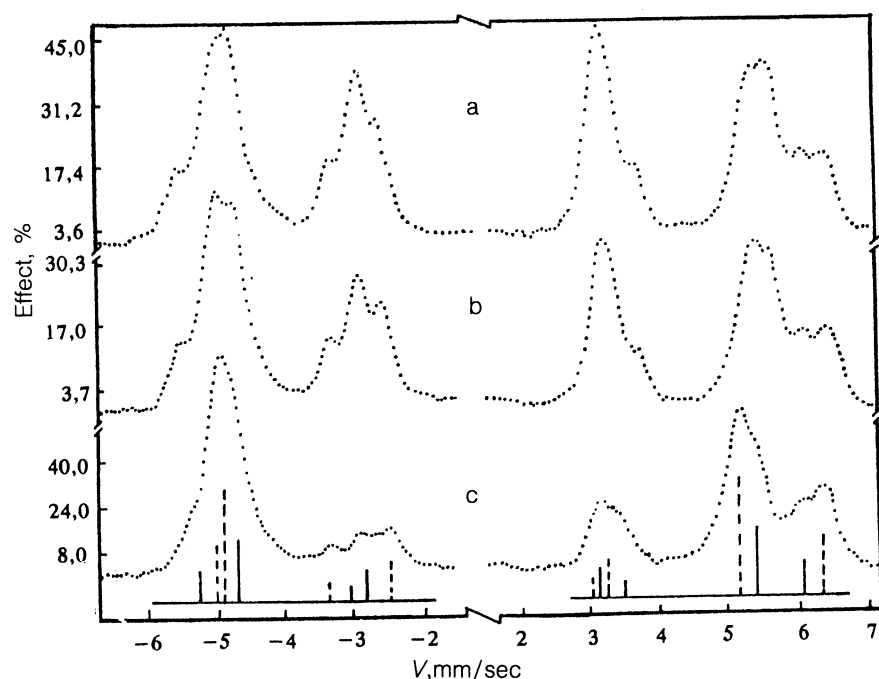


FIG. 10.  $\text{Fe}_3\text{BO}_6$  Mössbauer spectra obtained by recording electrons in the range 50–90 nm near  $T_R$  at temperatures of 415 K (a), 416 K (b), and 419 K (c).

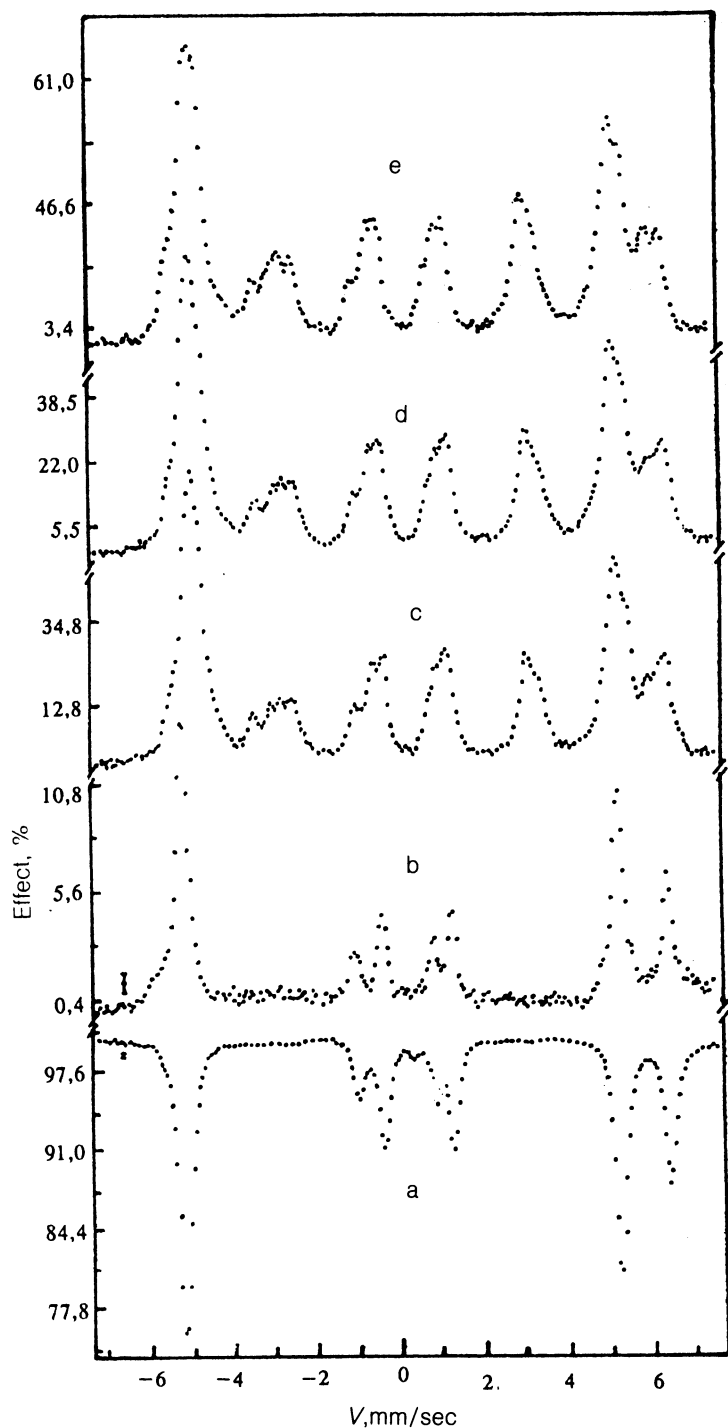


FIG. 11.  $\text{Fe}_3\text{BO}_6$  Mössbauer spectra obtained at  $T=417.1$  K by recording  $\gamma$ -rays (a), x-rays, (b), and electrons (c-e) from the interior (a,b) and surface layers from 0 to 40 nm (c), 50 to 90 nm (d), and 150 to 200 nm (e). The location and thickness of the layer is determined to within 20%.

temperatures from  $T_1$  to  $T_2$  these lines consist of components belonging to the  $\Gamma_2$  phase, and the second and fifth lines of the sextuplets corresponding to the  $\Gamma_3$  phase are absent.

The experimental Mössbauer spectra obtained in region III by recording the secondary electrons from layers lying at different depths from the surface of the crystal are displayed in Figs. 8b-d. Analysis shows that as the crystal surface is approached, the lines of the phase observed at  $T < T_1(L)$  become stronger, while the lines belonging to the phase observed at temperatures  $T > T_2(L)$  become

weaker. This is seen well for the second and sixth lines of the Zeeman sextuplets displayed in Figs. 8b-d.

The experimental spectra obtained from the surface layer lying 50 to 90 nm (the location and thickness of the layers are determined with an accuracy of 20%) from the crystal surface by recording secondary electrons at different temperatures from  $T_1(L)$  to  $T_2(L)$  are displayed in Fig. 10. As is evident from Fig. 10, the spectra consist of a superposition of Zeeman spectra, observed by recording electrons above  $T_2(L)$  and below  $T_1(L)$ . As the temperature increases from  $T_1(L)$  to  $T_2(L)$  the lines belonging

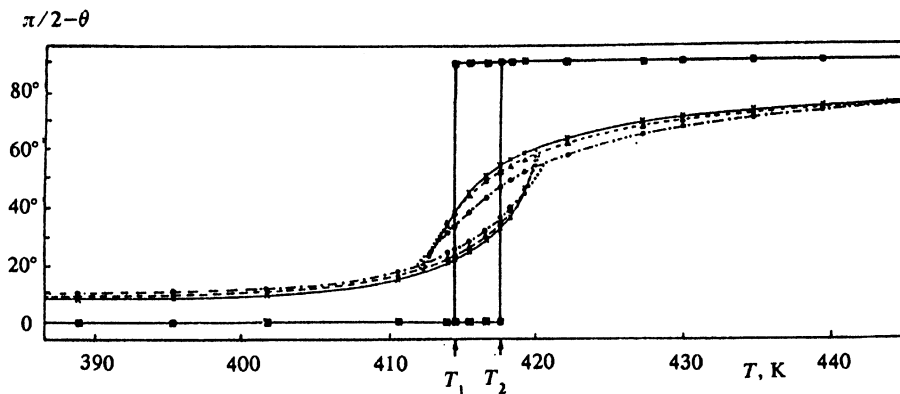


FIG. 12. Temperature dependences of the orientation angles  $\theta$  of spins in the interior (●) and surface layers of a  $\text{Fe}_3\text{BO}_6$  crystal. Layer thicknesses: 0 to 40 nm (●), 50 to 90 nm (▲), and 150 to 200 nm (×).

to the phase below  $T_1(L)$  become weaker and they vanish at  $T_2(L)$ . The lines belonging to the phase above  $T_2(L)$  appear at temperatures  $T_1(L)$ , and they become stronger as the temperature increases from  $T_1(L)$  to  $T_2(L)$ .

As the temperature increases further, one can see in the experimental spectra obtained by recording the  $\gamma$ - and x-rays and displayed in Figs. 11a and b that the second and fifth lines of the Zeeman sextuplets are absent. This indicates that the interior of the crystal has been transformed into the  $\Gamma_3$  phase. It is clearly seen in the secondary-electron Mössbauer spectra in Figs. 11c–e that spectra of both phases, observed on the surface below and above the transition region, coexist. This proves convincingly that in the region of the reorientational phase transition an inhomogeneous state, in which the volume of the crystal has transformed from the  $\Gamma_2$  into the  $\Gamma_3$  phase while regions with different spin orientation are present at the surface, i.e., spin reorientation on the crystal surface is not yet completed, is observed in the region of the reorientational phase transition.

## 5. ANALYSIS OF THE EXPERIMENTAL RESULTS

The angles  $\theta$  determining the direction of the spin magnetic moments with respect to the direction of the incident  $\gamma$ -rays, were found from the intensity ratios of the first and second (fifth and sixth) lines in the Zeeman sextuplets using Eq. (4). The temperature dependence of this angle for surface layers and the volume of the crystal is displayed in Fig. 12. It is evident from Fig. 12 that the angle  $\theta$ , determined from the  $\gamma$ - and x-ray Mössbauer spectra, i.e., in the volume of the crystal, assumes only the two values 0 and  $\pi/2$ . Thus the spin magnetic moments of the iron ions located in the bulk of the crystal are directed along the  $c$  axis in the  $\Gamma_2$  phase and along the  $a$  axis in the  $\Gamma_3$  phase.

At temperatures from  $T_1$  to  $T_2$  the magnetic moments of the iron ions in the bulk of the crystal are parallel to the crystallographic  $c$  axis (for domains in the  $\Gamma_2$  phase) and the  $a$  axis (for domains in the  $\Gamma_3$  phase) and they do not have other orientations. These results prove convincingly that spin reorientation in the volume of a  $\text{Fe}_3\text{BO}_6$  crystal occurs as a first-order phase transition. At temperatures from  $T_1$  to  $T_2$  an inhomogeneous state, i.e., a domain structure consisting of the magnetic phases  $\Gamma_2$  and  $\Gamma_3$ , is

observed. The magnetic moments in the region of the non-uniform state are directed in the domains along the  $a$  and  $c$  axes. Similar results were obtained in Ref. 14 in investigations of the volume properties of crystals by means of conventional Mössbauer spectroscopy.

The picture changes for layers lying at depths less than 300 nm. The magnetic moments in a surface layer less than 300 nm thick tilt away from the direction parallel to the crystallographic  $a$  axis. This is observed at temperatures significantly lower than the temperature  $T_1$  of the onset of  $G_x F_z \leftrightarrow G_z F_x$  reorientation in the bulk of the crystal. At temperatures below  $T_1(L)$  the tilt angle of the magnetic moments away from the  $a$  axis increases toward the crystal surface (see Fig. 12).

At temperatures from  $T_1(L)$  to  $T_2(L)$  reorientation of the magnetic moments in the surface layer occurs, as is evident from Fig. 12, by continuous rotation from one direction to another. The closer the observed layer is to the crystal surface, the more smoothly the reorientation occurs. After the phase transition is completed, the magnetic moments in a surface layer less than 300 nm thick are oriented not along the crystallographic  $c$  axis, but rather at a small angle with respect to this axis. At temperatures  $T > T_2(L)$  this tilt angle increases as the surface is approached. As the temperature increases from  $T_2(L)$ , the tilt angle of the spin moments from the  $c$  axis decreases, as is evident from Fig. 12.

The temperature dependence of the line intensity obtained for the high-temperature phase from the experimental spectra is displayed in Fig. 13, whence one can see that, within the experimental error, the change in the line intensities is linear. The limits of the temperature range of the spin-reorientation process and of the inhomogeneous state were determined by extrapolating to zero the temperature dependence of the line intensities of the high-temperature phase. The obtained phase diagram is displayed in Fig. 14. As is evident from Fig. 14, the temperature range of the spin-reorientational phase transition becomes wider as the surface is approached from layers located in the bulk of the crystal.

It should be noted that for samples obtained from different laboratories the width of the transition in the volume of the crystal varies from fractions of a degree to 10 K. This is probably a function of how the crystal is synthe-

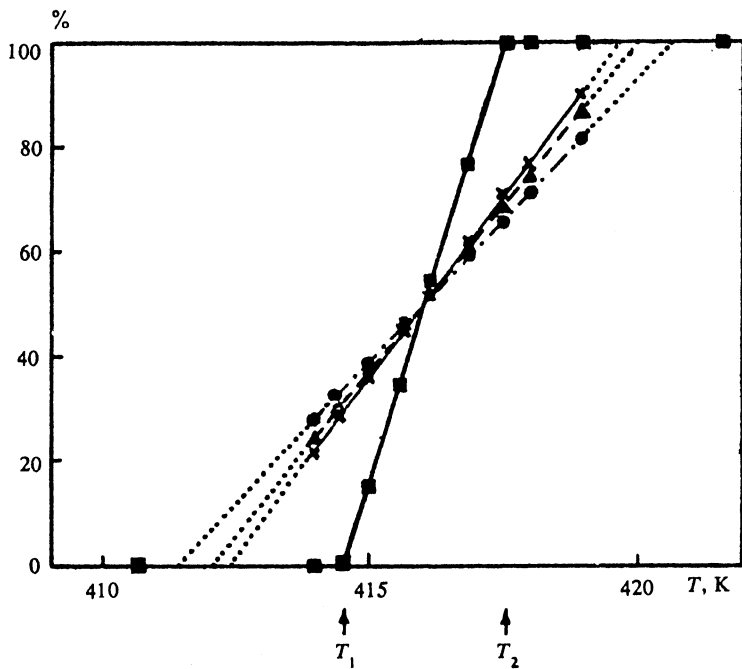


FIG. 13. Temperature dependence of the line intensity obtained for the high-temperature phase for the interior of the crystal (■) and surface layers. Layer thickness: 0 to 40 nm (●), 50 to 90 nm (▲), and 150 to 200 nm (×).

sized. The width of the transition at the surface of the experimental crystal varies in a manner similar to the width of the phase transition in the bulk sample.

Comparing the experimental results obtained by studying the reorientation of magnetic moments at the surface of a  $\text{Fe}_3\text{BO}_6$  crystal in which a first-order phase transition occurs in the interior shows that the results agree with the theory in which the direction of the easy axis at the surface is different from 0 or  $\pi/2$ . However, there is one difference. The theoretical investigations show that the temperature range of the surface transition is narrower than the transition in the volume (see Fig. 1b). It is evident from the experimental data that the temperature range of the phase transition becomes wider as the crystal surface is ap-

proached (Fig. 12). The explanation of this could lie in the fact that in the theoretical investigations<sup>16</sup> the reorientation in a ferromagnet was considered, whereas the experiments were performed in antiferromagnetic crystals.

## CONCLUSIONS

In conclusion we list the effects which have been established from the experimental data on spin-reorientational phase transitions at the surface and in the interior of an antiferromagnetic macrocrystal of  $\text{Fe}_3\text{BO}_6$ .

1. Phase transitions at the surface and in the interior of antiferromagnetic  $\text{Fe}_3\text{BO}_6$  macrocrystals were investigated by the method of simultaneous  $\gamma$ -ray, x-ray, and electron Mössbauer spectroscopy by recording radiations with different penetrating power. The spin reorientation process on the surface was described and a comparison was made to the transition mechanism operating in the interior of the macroscopic crystal.

2. In a surface layer less than 300 nm thick, outside the transition region, the magnetic moments at the surface are not collinear to the direction of the magnetic moments of the iron ions located in the interior of the crystal, but rather they are tilted by some angle. This tilt angle increases toward the surface of the crystal and toward the region of spin reorientation.

3. A first-order phase transition, accompanied by formation of a nonuniform state, occurs near the transition in the interior of the crystal. In a surface layer less than 300 nm thick reorientation occurs by continuous rotation of the magnetic moments away from directions along which they were oriented above and below the region of the spin-reorientational phase transition.

4. A nonuniform state, namely, domain structure, in which the directions of the magnetic moments differ not by

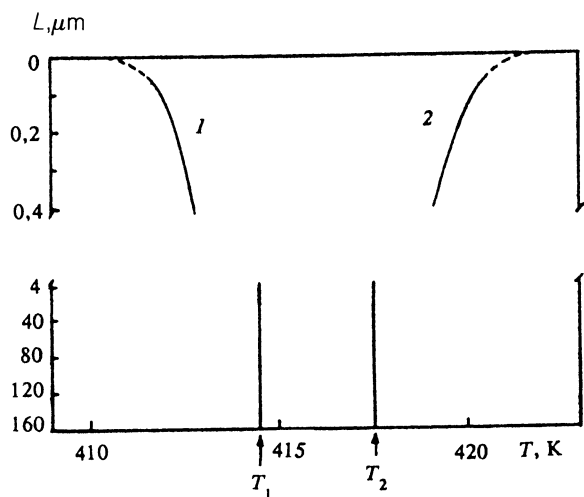


FIG. 14. Phase diagram of the states of  $\text{Fe}_3\text{BO}_6$  in the region of a spin-reorientation phase transition: 1—phase limit  $T_1(L)$ ; 2— $T_2(L)$ .

$\pi/2$ , as in the volume of the crystal, but rather by a smaller amount, is observed in a surface layer in the region of the transition. Thus the hysteresis loop on the surface of the crystal is narrower than in the interior. Further narrowing of the hysteresis loop is observed as the crystal surface is approached. It can be conjectured that the first-order phase transition observed in the interior of the  $\text{Fe}_3\text{BO}_6$  crystal transforms into a second-order transition in a layer which is located directly at the surface and whose thickness is less than that of the layer studied in the present work.

5. The transition temperature range becomes wider as the surface of the crystals approached from the interior of the crystal.

- <sup>1</sup>U. Gradmann, *J. Magn. Magn. Mater.* **100**, 481 (1991).
- <sup>2</sup>T. Shinjo, *Surf. Sci. Rep.* **12**, 49 (1991).
- <sup>3</sup>G. S. Krinchik, A. P. Khrebtov, A. A. Askochenskii, and V. E. Zubov, *Pis'ma Zh. Eksp. Teor. Fiz.* **17**, 466 (1973) [*JETP Lett.* **17**, 335 (1973)]; G. S. Krinchik and V. E. Zubov, *Zh. Eksp. Teor. Fiz.* **69**, 707 (1975) [*Sov. Phys. JETP* **42**, 359 (1976)].
- <sup>4</sup>V. E. Zubov, G. S. Krinchik, and V. A. Lyskov, *Zh. Eksp. Teor. Fiz.* **80**, 229 (1981) [*Sov. Phys. JETP* **53**, 115 (1981)].
- <sup>5</sup>E. A. Balykina, E. A. Tan'shina, and G. S. Krinchik, *Zh. Eksp. Teor. Fiz.* **93**, 1879 (1987) [*Sov. Phys. JETP* **66**, 1073 (1987)].
- <sup>6</sup>E. A. Balykina *et al.*, *Fiz. Tverd. Tela* **30**, 570 (1988) [*Sov. Phys. Solid State* **30**, 326 (1988)].
- <sup>7</sup>E. Boree and J. J. Hamman, *J. Phys.* **38**, 391 (1975).
- <sup>8</sup>V. G. Labushkin, V. V. Rudenko, and É. R. Sarkisov, *Pis'ma Zh. Eksp. Teor. Fiz.* **34**, 568 (1981) [*JETP Lett.* **34**, 544 (1981)].
- <sup>9</sup>V. E. Zubov *et al.*, *Zh. Eksp. Teor. Fiz.* **94**, 290 (1988) [*Sov. Phys. JETP* **67**, 2122 (1988)].
- <sup>10</sup>T. Shinjo *et al.*, *J. Magn. Magn. Mater.* **35**, 133 (1983).
- <sup>11</sup>O. Nikolov *et al.*, *Hyperfine Interactions* **39**, 409 (1988).
- <sup>12</sup>A. S. Kamzin, V. P. Rusakov, and L. A. Grigor'ev in *Proceedings of Physics of Transition Metals*, 1988, Part II, p. 271.
- <sup>13</sup>A. S. Kamzin and L. A. Grigor'ev, *Fiz. Tverd. Tela* **32**, 364 (1990) [*Sov. Phys. Solid State* **32**, 208 (1990)].
- <sup>14</sup>A. S. Kamzin, V. A. Bokov, and M. K. Chizhov, *Fiz. Tverd. Tela* **18**, 2795 (1976) [*Sov. Phys. Solid State* **18**, 1631 (1976)]; A. S. Kamzin and V. A. Bokov, *Fiz. Tverd. Tela* **19**, 2131 (1977) [*Sov. Phys. Solid State* **19**, 1247 (1977)].
- <sup>15</sup>K. P. Belov, A. K. Zvezdin *et al.*, *Oriental Transitions in Rare-Earth Magnetic Materials* [in Russian], Nauka, Moscow, 1979.
- <sup>16</sup>M. I. Kaganov, *Zh. Eksp. Teor. Fiz.* **79**, 1544 (1980) [*Sov. Phys. JETP* **52**, 779 (1980)].
- <sup>17</sup>M. I. Kaganov and A. V. Chubukov, *Zh. Eksp. Teor. Fiz.* **82**, 1617 (1982) [*Sov. Phys. JETP* **55**, 937 (1982)].
- <sup>18</sup>N. B. Ivanov and M. I. Kaganov, *Fiz. Tverd. Tela* **26**, 1101 (1984) [*Sov. Phys. Solid State* **26**, 669 (1984)].
- <sup>19</sup>A. S. Kamzin and L. A. Grigor'ev, *Pis'ma Zh. Tekh. Fiz.* **16**, 38 (1990) [*Sov. Tech. Phys. Lett.* **16**, 417 (1990)].
- <sup>20</sup>G. N. Belozerskii, *Mössbauer Spectroscopy as a Method for Investigation of Surfaces* [in Russian], Atomizdat, Moscow, 1990.
- <sup>21</sup>A. S. Kamzin and L. A. Grigor'ev, *Prib. Tekh. Eksp.*, No. 2, 74 (1991).
- <sup>22</sup>U. Gonser *et al.*, *Hyperfine Interactions* **66**, 95 (1991).
- <sup>23</sup>A. S. Kamzin *et al.*, *Prib. Tekh. Eksp.* No. 1, 80 (1993).
- <sup>24</sup>A. S. Kamzin and L. A. Grigor'ev, *Pis'ma Zh. Tekh. Fiz.* **19**, 8 (1993) (to be publ.).
- <sup>25</sup>V. S. Shpinel', *Mössbauer Effect in Crystals* [in Russian], Nauka, Moscow, 1969.
- <sup>26</sup>V. I. Gol'danskiĭ, L. I. Krizhanskiĭ, and V. V. Khrapov [eds.], *Applications of Mössbauer Spectroscopy in Chemistry* [Russian translation], Mir, Moscow, 1977.
- <sup>27</sup>J. G. White *et al.*, *Acta Cryst.* **19**, 1060 (1965).
- <sup>28</sup>R. Wolfe *et al.*, *Solid State Commun.* **7**, 949 (1969).
- <sup>29</sup>V. G. Bar'yakhtar *et al.*, *Pis'ma Zh. Eksp. Teor. Fiz.* **9**, 634 (1969) [*JETP Lett.* **9**, 391 (1969)].
- <sup>30</sup>A. S. Kamzin *et al.*, *Fiz. Tverd. Tela* **19**, 2030 (1977) [*Sov. Phys. Solid State* **19**, 1187 (1977)].
- <sup>31</sup>J. J. Johnson, *Hyperfine Interactions* **49**, 19 (1989).
- <sup>32</sup>G. J. Long, *Mössbauer Spectroscopy Applied to Inorganic Chemistry*, Plenum Press, New York, 1987, Vol. 2.
- <sup>33</sup>F. van der Woude, *Phys. Status Solidi* **36**, 1169 (1966).
- <sup>34</sup>A. N. Salugin *et al.*, *Fiz. Tverd. Tela* **16**, 1227 (1974) [*Sov. Phys. Solid State* **16**, 792 (1974)].

Translated by M. E. Alferieff